Ground Support 2026 - D Cumming-Potvin & J Wesseloo (eds.)
© 2026 Australian Centre for Geomechanics, Perth
doi:10.36487/ACG_repo/2625_17

Comparing steel mesh performance in an overlap condition

David Sweet [a,*], Tyler Emery [a], Samantha Wilson [a], Mary Humphreys [a]

[a] *Spokane Mining Research Division, National Institute of Occupational Safety and Health, USA*

Abstract

In pursuit of reducing incidents and injuries due to ground falls, the National Institute for Occupational Safety and Health (NIOSH) has expanded their novel high-energy, high-displacement (HEHD) test machine to test mesh ground support in an overlap condition. The overlap zone in overhead ground support is not widely tested but is seen as an area particularly vulnerable to damage as mesh is more likely to separate at this location rather than maintain its ability to take load. In this study, traditional steel mesh materials were tested in a quasi-static overlap condition with approximately 300 mm (12 in) of overlap. These materials were 9-gauge or 3.8 mm diameter chain link with a 50.8 mm (2 in) aperture, 6-gauge or 4.9 mm diameter welded wire mesh with 76 mm (3 in) aperture, and 6-gauge welded wire mesh with a 102 mm (4 in) aperture. Test results primarily showed a stiffening effect at the overlap, and the chain link displacement at the peak load decreased 34%, while both welded wire materials decreased by 41 to 52%. These results will improve industry understanding of mesh performance at the overlap zone by establishing what the relative peak load, material strain, and absorbed energy are. Understanding these relative properties will enable mine operators to further compare steel mesh materials.

Keywords: *ground support, mesh, liner, welded wire, chain link, overlap, mechanical performance, ground support*

1 Introduction

In underground mining, mesh is often used as overhead ground support between the main rockbolts or cables. Its function is to capture and hold loose rock that would otherwise fall into an excavation and potentially cause injury to personnel, damage to equipment, or delay in operations. Mesh is only one part of a ground control system that would also include reinforcement, such as rockbolts, connections such as bolt plates (Ortlepp 1983; Potvin et al. 2010), reinforced shotcrete, steel arches or cast-in-place concrete (Cai 2013). It is well known that the containment aspect of ground control is the weakest part of the system, and as expressed by Potvin et al. (2010), any ground support system is only as effective as its weakest link. Safety data from the Mine Safety and Health Administration shows that 27,520 ground control related incidents were reported between 2000 and 2021, resulting in injuries to 8,800 mine workers in the United States alone, of which 122 lost their lives and 65 were disabled (NIOSH 2024). As a result, the NIOSH has been researching the performance characteristics of different mesh materials to improve the safety of mines for mine workers. This portion of the study set out to better define the performance of mesh where it overlaps from piece to piece in a common bolting pattern. Currently, a test standard does not exist, so it is difficult to determine how mesh materials perform comparatively between different test apparatuses. Benton et al. (2022) sought to create and build upon a performance index that would compare different mesh materials relative to a standard material, chain link. This study seeks to expand this research effort following a similar methodology.

The overlap zone of overhead support where 2 mesh materials meet is not well understood. Typically, mesh is overlapped based on a minimum amount of material, such as 200 mm (8 in) to 300 mm (12 in), to help ensure it will not readily pull apart when loaded. Morkel et al. (2023) writes that the mesh overlap zone is seen as a common failure area, especially for welded wire and should be a focus area for further testing.

[*] Corresponding author. Email address: dsweet@cdc.gov

Cai (2013) also discusses that the connecting points are often the weakest link. Although some mesh testing has been conducted on the overlap zone (Brändle & Bucher 2023; Zhang & Eriksson 2023), it is clearly an area that requires more attention. Additional testing in this area will improve industry understanding of how mesh materials behave at the overlap zone and allow mine operators to make more informed decisions regarding ground control plans and improving occupational safety in underground mining.

2 Methodology

This study utilised the novel high-energy, high-deformation (HEHD) load frame that was designed by the NIOSH Spokane Mining Research Division (SMRD). Initially designed for testing large shotcrete panels (Benton et al. 2016), this load frame was later retrofitted with a larger stroke ram to enable testing of other overhead ground support (Benton et al. 2022). This load frame was designed based on Kirsten and Labrum's 1990 test setup (Kirsten & Labrum 1990).

Since the last published testing by Benton (Benton et al. 2022) the HEHD test machine was retrofitted with an upgraded hydraulic system and a steel frame with additional mounting locations. The machine works by using a hydraulic ram to press a loading head against a secured piece of ground control mesh. The mesh is secured using rockbolt plates and nuts. There is a high-capacity loadcell located under the hydraulic ram that reads the load applied to the mesh material. There is also a linear displacement transducer attached to the loading head and secured to the testing platform that reads the travel distance of the ram. Figure 1 shows a conceptual diagram of the HEHD with the upgraded components. The hydraulic upgrades include replacing the single-action, 3-stage, 600 mm (24 in) stroke, 1,500 kN (150 tonnes) capacity hydraulic ram with a dual-action, single-stage, 1,200 mm (48 in) stroke, 2,000 kN (200 tonnes) capacity ram. The 3-stage hydraulic ram used previously had an incrementally increasing displacement rate as the test progressed through each ram stage. By using a single-stage hydraulic ram, the tests were completed at a constant displacement rate of 9.6 mm/s (0.38 in/s). The upgraded stroke length ensures each sample reaches failure.

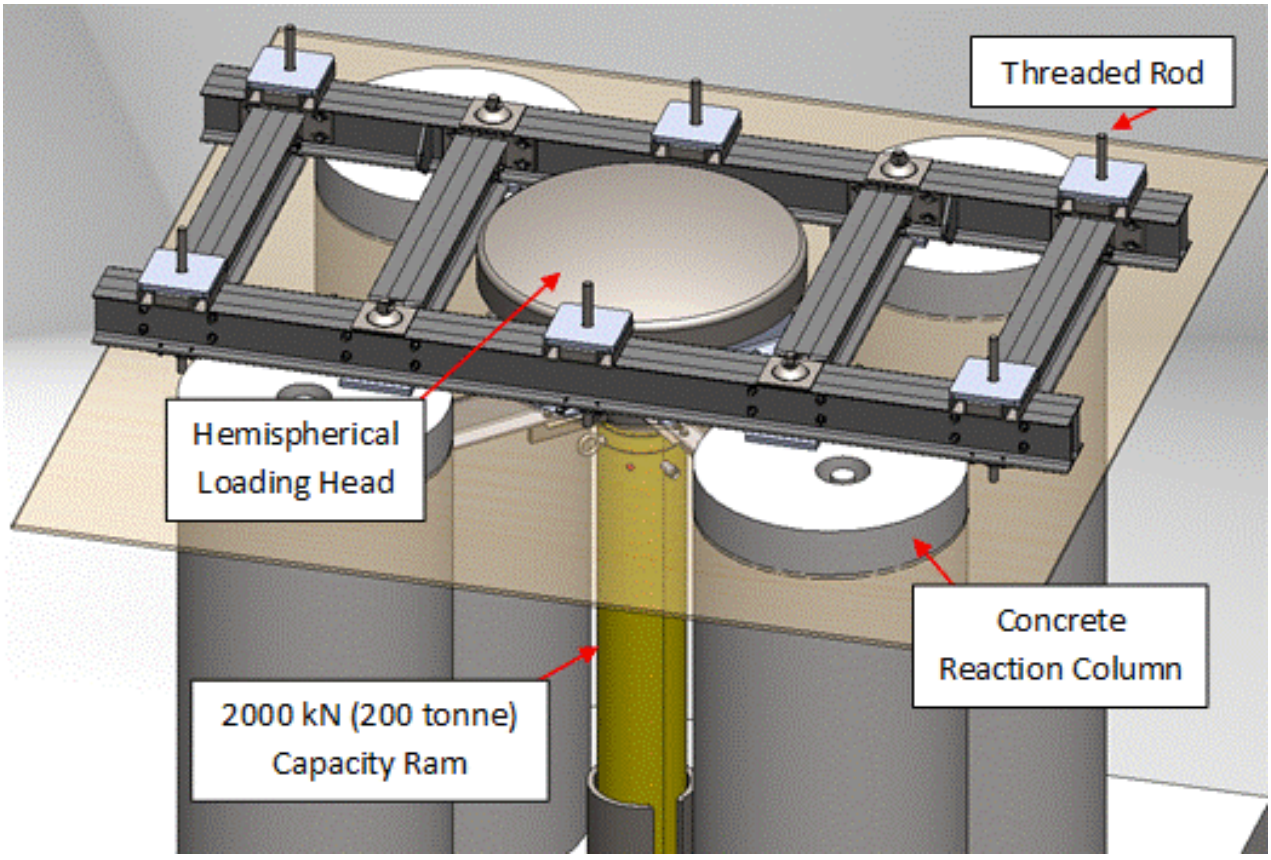
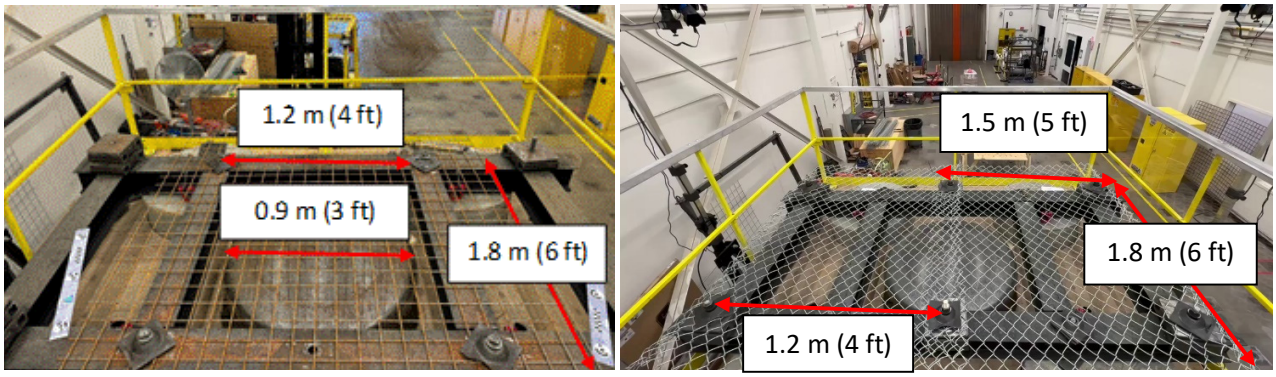


Figure 1 Model of upgraded high-energy, high-displacement test frame identifying key components (Credit: NIOSH)

The additional steel frame was designed and fabricated by SMRD to accommodate multiple testing configurations such as the standard case of loading a single mesh panel in the centre of the bolting pattern (single mesh test), as well as loading 2 mesh panels with the overlap centred to the loading head (overlapped mesh test). The bolt pattern remained 1.2 × 1.2 m (4 × 4 ft) for both setups. Figure 2a shows the setup for single mesh tests where the original rockbolts are used to secure the sample. For the overlapped mesh tests, 6 threaded rods are inserted into alternate bolt locations as shown in Figure 2b.



(a) (b)

Figure 2 Images of test setups with dimensions. (a) Image of a single mesh test setup for 76 mm (3 in) aperture welded wire. The hemispherical loading head is 0.9 m (3 ft) in diameter. The mesh panels are cut to 1.8 by 1.8 m (6 by 6 ft). Bolt spacing is 1.2 m (4 ft); (b) Image of overlapped mesh test setup for chain link. The mesh panels are cut to 1.5 by 1.8 m (5 by 6 ft). Bolt spacing is 1.2 m (4 ft) for each panel (Credit: NIOSH)

This study focuses testing on 3 materials that are commonly used in industry for overhead ground support:

- chain link, 50.8 mm (2 in) aperture, 3.8 mm wire diameter (9-gauge)
- welded wire, 76 mm (3 in) aperture, 4.9 mm wire diameter (6-gauge)
- welded wire, 102 mm (4 in) aperture, 4.9 mm wire diameter (6-gauge).

The primary focus for this study is comparing the mechanical properties of the mesh material as tested on a 1.2 × 1.2 m (4 × 4 ft) bolt pattern to an overlap test where 2 mesh panels are overlapped close to 300 mm (12 in).

An additional parameter tested during this study was alternating the welded wire panels such that the cross wires interlocked at the overlap zone, shown in Figure 3. This was to see if there was a strength increase by intentionally creating an interlock between the materials.

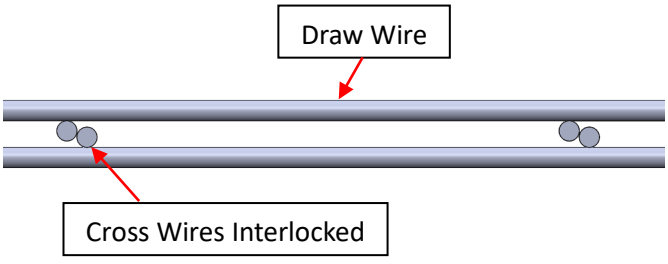
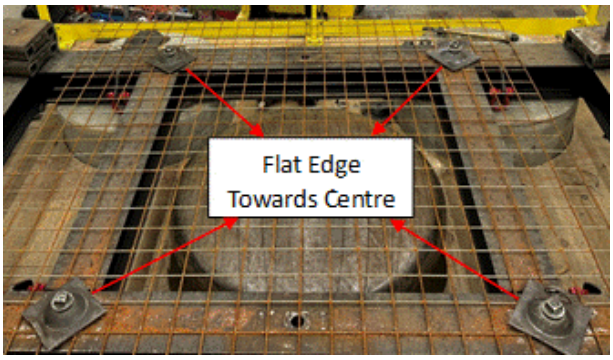
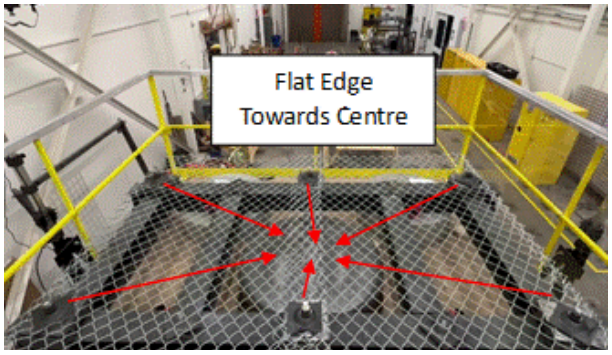


Figure 3 Modelled side view of alternated welded wire panels to induce interlocking of the cross wires for one series of overlap tests (series O-WW4-CWA-S). Draw wires are shown lengthwise across the model and the cross wires are shown interlocked (Credit: NIOSH)

All samples for the standard single mesh tests were cut to 1.8 × 1.8 m (6 × 6 ft) and all samples for the overlap mesh tests were cut to 1.5 × 1.8 m (5 × 6 ft). The overlap test samples were cut shorter to ensure the guard railing did not interfere with the sample installation. For each test, the steel bolt plates were oriented such that a flat edge faced towards the loading ram, shown in Figure 4a and b below. This was to reduce the effect of a point load from the plates to the mesh material.



(a)



(b)

Figure 4 Images showing flat edge of bolt plates oriented towards centre of loading head for (a) single mesh tests and (b) overlap mesh tests (Credit: NIOSH)

All samples were attached to the test frame using 4 threaded rods for the single mesh tests and 6 threaded rods for the overlap tests. The nuts were torqued to 150 Nm (110 ft-lbs) using a ratcheting torque wrench. This constraining method was used to closely mimic in situ conditions.

As reported by Benton et al. (2022), chain link was selected as a standard to compare other materials against. In this study, the averaged chain link results obtained from the single mesh tests (i.e. CL-S series) were used as the comparative standard. In doing so, industry will have a means to compare these materials and their overlap zones.

In all, 57 tests were completed investigating seven different configurations which are shown in Table 1 below. The data collected in each test includes the peak load, the absorbed energy at the peak load ('Energy at Peak'), the displacement at the peak load ('Disp. at Peak'), and the absorbed energy at 500 mm (20 in) of displacement ('Energy at 500 mm'). The table displays the number of samples tested in each series in column 'Tests'. Initially, 10 samples from each configuration were tested, but as the study progressed additional configurations were added leading to a lower sample count in certain series. The percent coefficient of variation (CV) was calculated for each of the averages by dividing the standard deviation (σ) by the mean (μ) and multiplying by 100. This is shown in Equation 1.

$$CV = \frac{\sigma}{\mu} \times 100 \quad (1)$$

The CV shows the amount of variation relative to the mean of each parameter and is shown in Table 1 in parenthesis under each averaged value.

Table 1 Averaged data and coefficient of variation (%) for each test series including peak load, absorbed energy at peak load (Energy at peak), displacement at peak load (Disp. at peak), absorbed energy at 500 mm of displacement (Energy at 500 mm), and the number of tests completed

Series	Material	Average peak load (kN)	Average energy at peak (kJ)	Average disp. at peak (mm)	Average energy at 500 mm (kJ)	Total number of tests
CL-S	Chain link (50.8 mm, 9-gauge)	57 (12%)	9 (16%)	629 (4%)	4 (9%)	10
O-CL-S	Chain link (50.8 mm, 9- gauge), overlap	86 (9%)	10 (13%)	414 (4%)	14 (8%)	10
WW3-CWD-S	Welded wire (76 mm, 6- gauge), cross wires down	54 (4%)	6 (29%)	404 (13%)	9 (5%)	10
O-WW3-CWD-S	Welded wire (76 mm, 6-gauge), cross wires down, overlap	53 (13%)	3 (30%)	194 (10%)	11 (9%)	7
WW4-CWD-S	Welded wire (102 mm, 6-gauge), cross wires down	38 (11%)	5 (33%)	461 (20%)	6 (10%)	10
O-WW4-CWD-S	Welded wire (102 mm, 6-gauge), cross wires down, overlap	37 (17%)	3 (46%)	228 (24%)	8 (11%)	5
O-WW4-CWA-S	Welded wire (102 mm, 6- gauge), cross wires alternating, overlap	34 (20%)	3 (83%)	274 (57%)	7 (15%)	5

3 Results

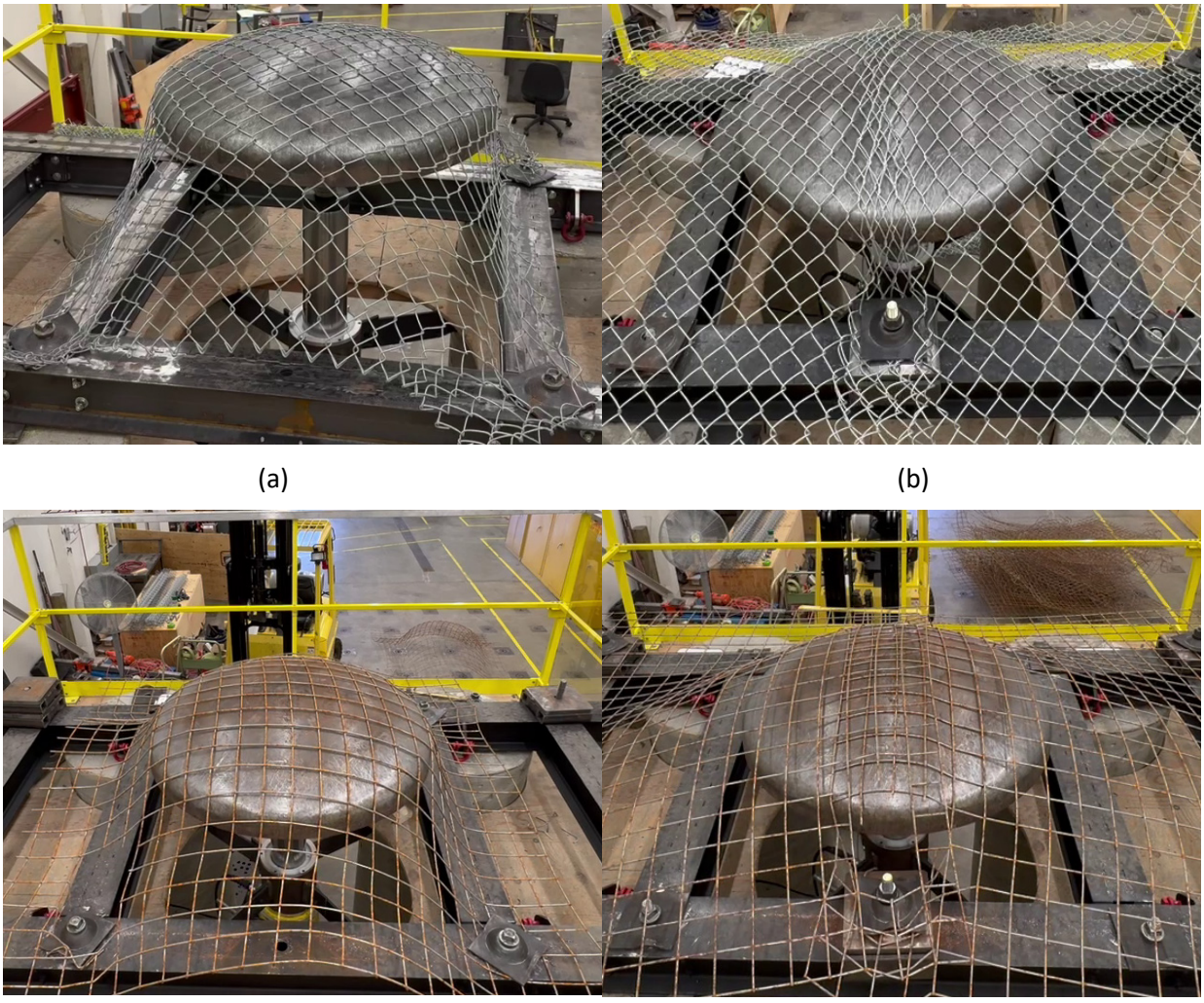
The chain link material showed the least amount of variation across the energy at peak load and the displacement at peak load while the 76 mm (3 in) welded wire mesh showed the least variation across the peak load and absorbed energy at 500 mm of displacement. The 102 mm (4 in) welded wire mesh accounted for the largest variation of all testing parameters; peak load, energy at peak load, displacement at peak load and energy at 500 mm of displacement. The CV ranged from 11 to 83% for this material, although this was likely due to a smaller sample size for the overlap tests.

The highest averaged values for peak load were from the overlapped chain link (O-CL) series at 86 kN (19,300 lbs). This test series also showed the highest averaged values for the energy absorbed at peak load and at 500 mm (20 in) of displacement, 10 and 14 kJ respectively. The standard chain link (CL) test series demonstrated the largest displacement at peak load of 629 mm (24.7 in).

The lowest averaged peak load was seen in the overlapped 102 mm (4 in) welded wire test series with alternated panels (O-WW4-CWA-S) at 34 kN (7,600 lbs). The overlapped welded wire test series (O-WW3-CWD-S, O-WW4-CWD-S, and O-WW4-CWA-S) accounted for the lowest values for energy absorbed at peak load and the displacement at peak load. The least average displacement at peak load was from the overlapped 76 mm (3 in) welded wire series (O-WW3-CWD-S) at 193 mm (7.6 in) of displacement. The lowest absorbed energy at peak load was from the overlapped 76 mm (3 in) welded wire (O-WW3-CWD-S) and both 102 mm (4 in) welded

wire overlapped series (O-WW4-CWD-S and O-WW4-CWA-S) which had an average of 3 kJ. However, the lowest absorbed energy at 500 mm of displacement was from the CL-S series which had an average of 4 kJ.

The near-failure high-stress state of select mesh tests, both single and overlapped, is shown below in Figures 5a–d. The CL material wires are loaded in the axial direction due to the diamond shape of the apertures while the wires on the welded wire mesh are loaded diagonally due to the orientation of the wires. The failure mechanisms for each differed. The CL material primarily failed due to the wires breaking in tension. The welded wire material primarily failed at the welded joints either in the heat affected zone or directly at the weld.



(a) (b)

(c) (d)

Figure 5 Near-failure images to demonstrate heavy loading of (a) single chain link, (b) overlapped chain link, (c) single 76 mm welded wire, and (d) overlapped 76 mm welded wire. Credit: NIOSH

4 Discussion

To better understand how the overlap tests compared to the single mesh tests (e.g. compare O-CL-S to CL-S) a percentage comparison was calculated based on the standard test. This was calculated by dividing the difference of the overlap test results, o, minus the standard test results, s, by the standard test result. This is shown in Equation 2 below:

$$\frac{(o-s)}{s} \times 100 \quad (2)$$

Positive values indicate a percent increase while negative values indicate a percent decrease.

In addition, a 2-sample t-test compared the means of each test series to determine which has a statistical difference. A t-test gives a p-value for each set of standard and overlap tests, which indicates whether there is a statistical difference between tests. The p-value in this study is evaluated at an alpha level of 0.05.

Table 2 below shows the percentage comparison and identifies which results showed a statistical difference, noted by the '*' symbol.

Table 2 Mesh test performance comparing the averaged data for each overlap test series to the corresponding standard single mesh test series (absorbed energy at peak load = Energy at peak, displacement at peak load = Disp. at peak, absorbed energy at 500 mm of displacement = Energy at 500 mm)

Series comparison	Material	Peak load	Disp. at peak	Energy at peak	Energy at 500 mm
CL-S	Chain link (50.8 mm, 9-gauge)	*52%	*−34%	*16%	*287%
O-CL-S	chain link (50.8 mm, 9-gauge), overlap				
WW3-CWD-S	welded wire (76 mm, 6-gauge), cross wires down	−3%	*−52%	*−56%	*16%
O-WW3-CWD-S	welded wire (76 mm, 6-gauge), cross wires down, overlap				
WW4-CWD-S	welded wire (102 mm, 6-gauge), cross wires down	−1%	*−51%	*−51%	27%
O-WW4-CWD-S	welded wire (102 mm, 6-gauge), cross wires down, overlap				
WW4-CWD-S	welded wire (102 mm, 6-gauge), cross wires down	−10%	*−41%	*−41%	14%
O-WW4-CWA-S	welded wire (102 mm, 6-gauge), cross wires alternating, overlap				

'*' indicates t-test p-value was less than 0.05 indicating standard and overlapped tests were statistically different

The overlap tests showed a reduction in displacement at peak load, which can be interpreted as an increase in stiffness, for all materials when compared to the standard single mesh tests. The welded wire materials had a higher increase in stiffness at peak load for the overlap tests compared to the CL. For CL, the overlap tests averaged a 34% increase in stiffness at peak load, while the 76 mm (3 in) welded wire material showed an increase in stiffness at peak load of 52%. The 102 mm (4 in) welded wire showed about the same increase as the 76 mm (3 in) welded wire at 51 and 41% for overlap and alternated overlap (O-WW4-CWD-S and O-WW4-CWA-S) respectively.

In terms of changes in peak load at the overlap, the CL material behaved differently than both the welded wire materials. The chain link showed a peak load increase of 52% (O-CL-S), while the 76 mm (3 in) welded wire (O-WW-CWD-S) showed a decrease of 3%, and the 102 mm (4 in) welded wire showed a decrease of 1 and 10% for regular overlapped tests and overlap tests with the cross wires alternated (O-WW4-CWD-S and O-WW4-CWA-S respectively). During overlap testing, the CL material interlocked over the loading head because of the higher profile woven design. This is likely what caused the CL material to exhibit higher peak loads. The overlapped, alternated 102 mm (4 in) welded wire tests (series O-WW4-CWA-S) were intentionally interlocked via the cross wires, yet the results indicated a strength loss rather than a strength gain, more so than the non-interlocked overlap mesh tests. The change in peak load for all welded wire materials at the overlap was not statistically different compared to the standard single mesh tests. Thus, there is no appreciable change in peak load at the overlap for the welded wire materials.

The absorbed energy at peak load was different for the CL and welded wire materials when loaded at the overlap as well. In addition, all comparison results for the energy at peak load were found to be statistically different. The chain link material showed an increase of 16% (O-CL-S), while the welded wire materials all showed a decrease. The 76 mm (3 in) welded wire mesh (O-WW3-CWD-S) decreased 56% and the 102 mm (4 in) aperture welded wire mesh decreased 51%, and 41% for the overlapped and alternated overlapped tests respectively (series O-WW4-CWD-S and O-WW4-CWA-S). The CL material displayed an increased capacity to absorb energy when loaded at the overlap zone, while the capacity of the welded wire mesh decreased. This effect was reduced by interlocking the cross wires (i.e. O-WW4-CWA-S versus O-WW4-CWD-S series).

The change in each material's energy absorption at 500 mm (20 in) of displacement was more varied. Again, the CL material showed a very different result than the welded wire materials. At 500 mm (20 in) of displacement, the overlapped CL series showed a significant increase in absorbed energy of 287%. The 76 mm (3 in) welded wire showed an increase of 16% when loaded at the overlap, and the 102 mm (4 in) welded wire series showed an increase of 27 and 14% for O-WW4-CWD-S and O-WW4-CWA-S, respectively. It is important to note that not all samples in either of the 102 mm (4 in) welded wire overlapped series (O-WW4-CWD-S and O-WW4-CWA-S) reached 500 mm (20 in) of displacement. As a result, the absorbed energy at 500 mm (20 in) of displacement for the 102 mm (4 in) welded wire series was not statistically significant. Additional tests should be conducted to verify if there is a statistical difference between these series.

To better illustrate the results, a representative sample was selected from each test series and used for comparison graphically. Figure 6 is a graph of the load versus displacement and absorbed energy versus displacement for the CL tests. The graph depicts a decrease in displacement (increase in stiffness) and an increase in peak load compared to the standard single mesh test. At 500 mm (20 in) of displacement, the overlap tests are already past the peak load, while the standard single mesh tests are still before the peak. In addition, the shape of the curve is steeper for the overlap tests both in the initial loading phase as well as in the failure zone. The absorbed energy versus displacement data for the CL material can also be seen in Figure 6. Most of the absorbed energy for the overlapped test is realised at about 600 mm of displacement, whereas the standard single mesh test shows a gradual gain until about 1,100 mm of displacement.

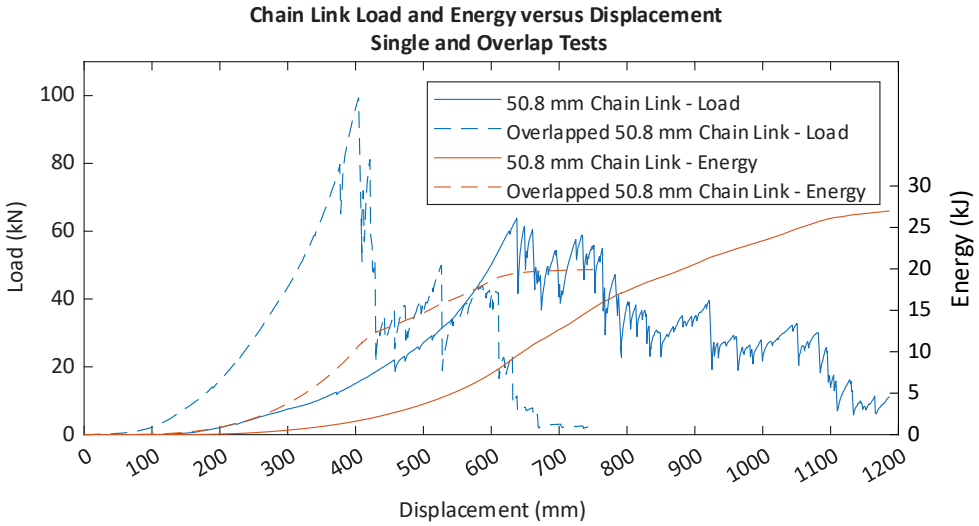
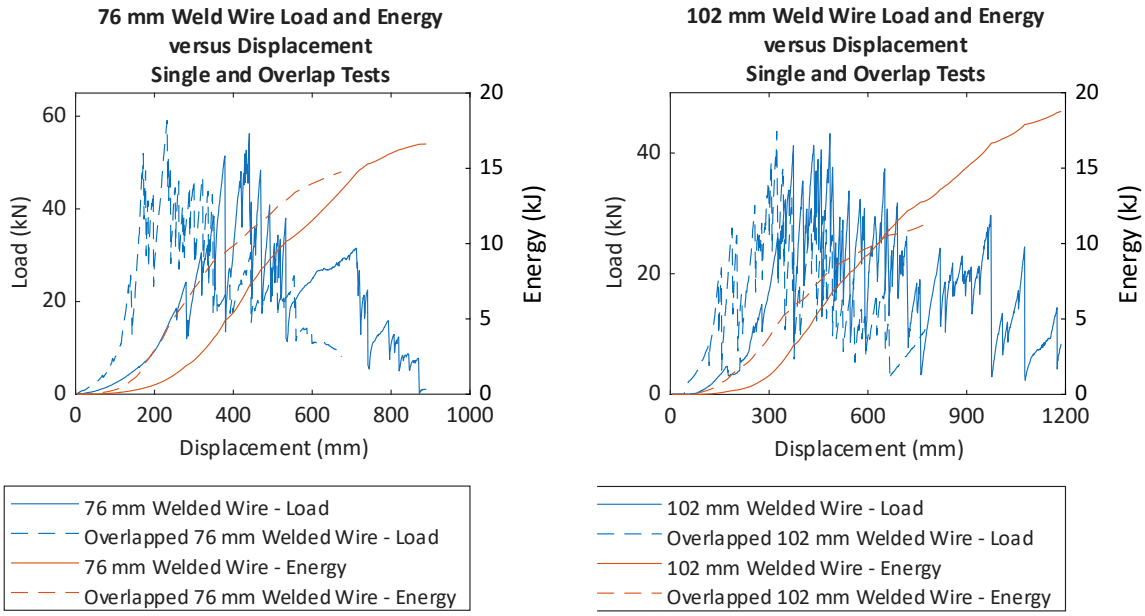


Figure 6 Load versus displacement and absorbed energy versus displacement of representative samples from chain link mesh test series (CL-S and O-CL-S)

The 76 mm (3 in) welded wire series is graphed in Figure 7a, and the 102 mm (4 in) welded wire series is graphed in Figure 7b. The overlap tests show a steeper loading curve and a horizontal shift towards increased stiffness (shorter displacement) compared to the standard single mesh tests. The absorbed energy versus displacement curves also shows a horizontal shift to shorter displacement with only a small difference seen for the 6-gauge, 102 mm (4 in) aperture welded wire material. The welded wire materials slid apart and had

low flexibility at the overlap compared to the CL because the wires are directly loaded, whereas the CL is pre-bent and deforms as the material is loaded. This is likely why the performance results differ.



(a) (b)

Figure 7 Load versus displacement and absorbed energy versus displacement of representative samples from (a) 76 mm (3 in) welded wire mesh test series (WW3-CWD-S and O-WW3-CWD-S) and (b) from 102 mm (4 in) welded wire mesh test series (WW4-CWD-S and O-WW4-CWD-S)

Figure 8 graphs the load and absorbed energy results from a representative sample from both 102 mm (4 in) welded wire overlap tests. The alternated welded wire tests show a higher initial peak load, yet the load and energy curves still closely follow the same trend.

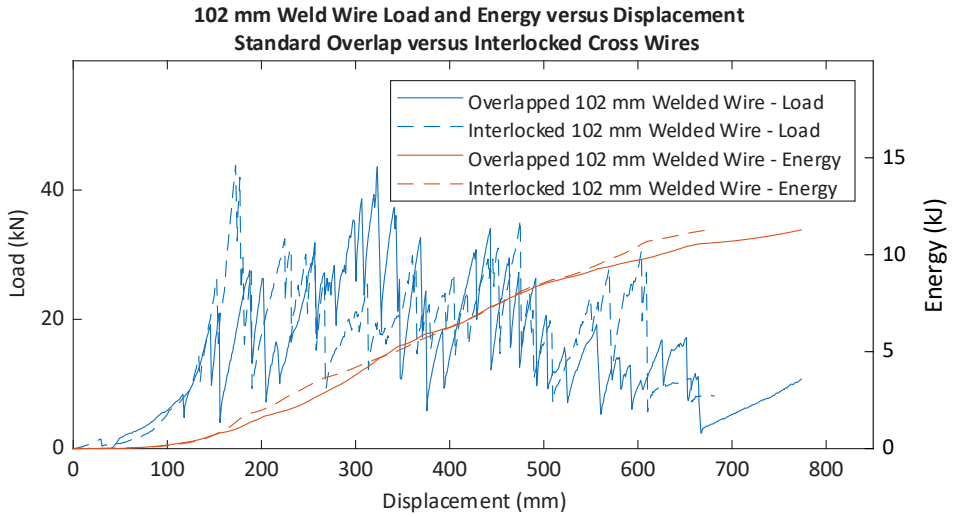
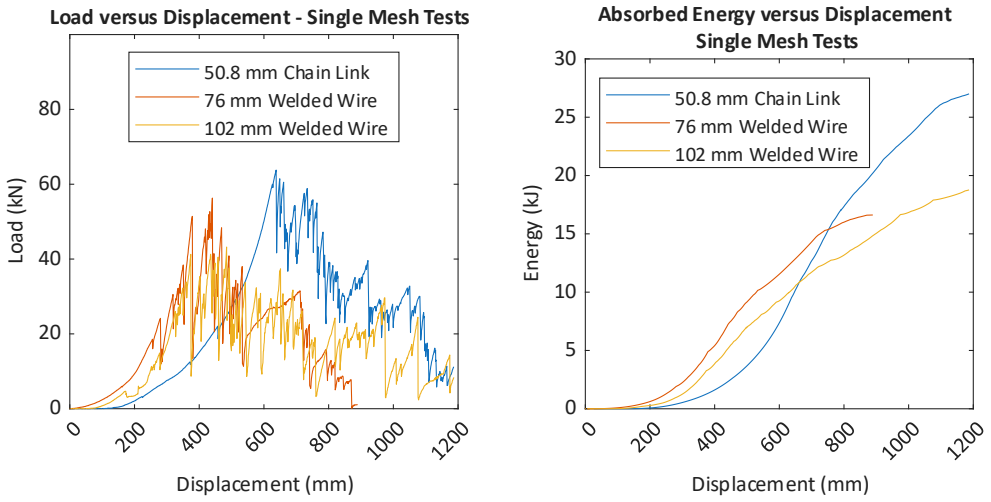


Figure 8 Load versus displacement and absorbed energy versus displacement of representative samples from the two 102 mm (4 in) welded wire overlapped mesh test series

Comparing the standard tests for all 3 materials, referencing Table 1 above, the CL demonstrated the highest value for peak load, displacement at peak load, and absorbed energy at peak load; 57 kN (12,800 lbs), 629 mm (25 in), and 9 kJ respectively. The 6-gauge, 76 mm (3 in) welded wire showed the highest absorbed energy at 500 mm (20 in) of displacement at 9 kJ. The welded wire materials decreased in peak load as the aperture size increased. The opposite was true for the displacement at peak load. The cumulative effect was

that as the aperture size increased the energy the sample was able to absorb at peak load as well as at 500 mm (20 in) of displacement was reduced. Load versus displacement and absorbed energy versus displacement results are displayed in Figure 9a and b respectively.



(a) (b)

Figure 9 Graphs of representative samples from the standard single mesh test series for each material showing (a) Load versus displacement data and (b) absorbed energy versus displacement data

The comparative concept initiated by Benton et al. (2022) was mimicked with these mesh test results in Table 3. In this table, all materials and configurations are compared to the averaged standard single mesh CL test result. This is set as a standard in order to show relative performance. Each test is calculated into a percentage relative to the CL material.

Table 3 Mesh test performance data comparing the averaged data for each test series to the standard single mesh chain link series (CL-S) (absorbed energy at peak load = Energy at peak, displacement at peak load = Disp. at peak, absorbed energy at 500 mm of displacement = Energy at 500 mm)

Series	Material	Peak load (kN)	Energy at peak (kJ)	Disp. at peak (mm)	Energy at 500 mm (kJ)
CL-S	Chain link (50.8 mm, 9-gauge)	100%	100%	100%	100%
O-CL-S	Chain link (50.8 mm, 9-gauge), overlap	152%	116%	66%	387%
WW3-CWD-S	Welded wire (76 mm, 6-gauge), cross wires down	96%	69%	64%	250%
O-WW3-CWD-S	Welded wire (76 mm, 6-gauge), cross wires down, overlap	93%	30%	31%	290%
WW4-CWD-S	Welded wire (102 mm, 6-gauge), cross wires down	66%	59%	73%	164%
O-WW4-CWD-S	Welded wire (102 mm, 6-gauge), cross wires down, overlap	66%	28%	36%	209%
O-WW4-CWA-S	Welded wire (102 mm, 6-gauge), cross wires alternating, overlap	60%	34%	44%	187%

5 Conclusions

Overall, the CL material (including the overlap tests) accounted for the highest averaged values for each of the calculated parameters listed below:

- peak load
- energy at peak load
- displacement at peak load
- energy at 500 mm (20 in) of displacement.

The lowest averaged peak load was seen in the 6-gauge, 102 mm (4 in) welded wire overlap test series that alternated the cross wires (O-WW4-CWA-S). The lowest displacement at peak load and absorbed energy at peak load were concentrated in the overlap tests for both welded wire materials. The lowest energy absorbed at 500 mm (20 in) of displacement was from the CL single mesh tests.

Looking at the overlapped test series, all materials exhibited a stiffer response characterised by a steeper load versus displacement curve, in addition to a negative shift in displacement, when tested in the overlap condition:

- 34% for CL tests
- 41–52% for welded wire tests.

Due to the increase in stiffness with the overlap tests, the absorbed energy at 500 mm (20 in) was increased, especially for the CL material, signifying not only a higher load capacity but also a reduced strain capacity. The CL showed a 52% increase in peak load when tested in the overlap condition, while the welded wire materials did not show a substantial change in peak load. The absorbed energy at 500 mm (20 in) of displacement substantially increased for the CL material at 287% when tested in the overlap condition. The absorbed energy at 500 mm (20 in) of displacement increased for the welded wire material between standard and overlapped tests, from 14 to 27%; however, multiple welded wire samples did not reach 500 mm (20 in) of displacement, so additional tests should be conducted to verify these results.

Focusing on the standard single mesh tests, the CL showed the highest value for peak load, displacement at peak load, and energy absorbed at peak load:

- peak load: 57 kN (12,800 lbs)
- displacement at peak: 629 mm (25 in)
- energy absorbed at peak: 9 kJ.

The 6-gauge, 76 mm (3 in) welded wire mesh showed the highest average absorbed energy at 500 mm (20 in) of displacement at 9 kJ. As the aperture size decreased the mesh exhibited a stiffer response (i.e. peak load increases and displacement at peak load decreases).

Testing the 6-gauge, 102 mm (4 in) welded wire mesh in the cross wires alternated position for overlap tests (O-WW3-CWA-S series) showed a similar response when compared to the regular overlap tests. The peak load showed a larger decrease of 10% for the O-WW4-CWA-S series compared to the standard tests (WW4-CWD-S), whereas there was only a 1% decrease for the non-alternated series (O-WW4-CWD-S). The change in displacement at peak load was less for the alternated samples showing a 41% reduction, while the non-alternated samples had a 51% reduction compared to the standard tests. The energy at peak load decreased 41% for the alternated samples and decreased 51% for the non-alternated samples compared to the single mesh test series. The energy at 500 mm (20 in) of displacement for the alternated samples showed an increase of 14%, while the non-alternated samples showed an increase of 27%. Additional tests should be conducted in these series as only 2 samples from each reached 500 mm (20 in) of displacement.

6 Future research

Due to the modifications to the HEHD test machine, NIOSH researchers will pursue testing synthetic mesh materials such as polyethylene terephthalate and combination polyester and polyvinyl chloride. Additional materials and combinations will be investigated to further develop a performance comparison table.

While this study focuses on quasi-static test results, which are representative of high-strain ground conditions, additional research with similar testing parameters implemented under dynamic conditions would also be beneficial. This would provide industry with performance results for high ground movement and high-energy ground conditions.

Supplementary test modifications are under consideration to build a better understanding of the correlation of performance to material and test configurations. Possible modifications include adjusting the size of the loading head based on the aperture size of the mesh material, testing the mesh over a series of load head sizes, increasing the friction at the bolt and load head locations to better mimic rock surfaces, and using a rock surface texture at the loading head instead of the steel round dome.

Currently, industry lacks a testing standard for quantifying the performance of overhead ground support. Proper selection should consider not only the mechanical performance of the material, but all facets of ground support selection and design, such as the material's resistance to corrosion, flammability, personnel safety and capacity for impact damage.

Acknowledgement

The authors thank Steve Murray and Greg Feagan of SMRD for their assistance with mesh preparation and testing, and Paul Janson and Mark Powers for setting up the electronics and operating data collection.

Disclaimer

The findings and conclusions in this report are those of the author(s) and do not necessarily represent the official position of the National Institute for Occupational Safety and Health, Centres for Disease Control and Prevention.

References

Benton, D, Iverson, S, Martin, L, Johnson, J & Raffaldi, M 2016, 'Volumetric measurement of rock movement using photogrammetry', *International Journal of Mining Science and Technology*, vol. 26, no. 1, pp. 123–130.

Benton, DJ, Sweet, DJ & Emery, TM 2022, 'Comparative analysis of synthetic and steel mesh performance', in *Proceedings of the 56th US Rock Mechanics/Geomechanics Symposium*, American Rock Mechanics Association, Westminster.

Brändle, R & Bucher, R 2023, 'Large-scale tests of weld mesh versus high-tensile chain link mesh on mesh overlap load transfer', in J Wesseloo (ed.), *Ground Support 2023: Proceedings of the 10th International Conference on Ground Support in Mining,* Australian Centre for Geomechanics, Perth, pp. 399–410, https://doi.org/10.36487/ACG_repo/2325_26

Cai, M 2013, 'Principles of rock support in burst-prone ground', *Journal of Tunnelling and Underground Space Technology*, vol. 36, pp. 46–56.

Kirsten, HAD & Labrum, PR 1990, 'The equivalence of fibre and mesh reinforcement in the shotcrete used in tunnel-support systems', *Journal of the South African Institute of Mining and Metallurgy*, vol. 90, pp. 153–171.

Morkel, IG, Mikula, PA & Whiting, RK 2023, 'A review of ground support mesh testing around the world', in J Wesseloo (ed.), *Ground Support 2023: Proceedings of the 10th International Conference on Ground Support in Mining*, Australian Centre for Geomechanics, Perth, pp. 373–398, https://doi.org/10.36487/ACG_repo/2325_25

NIOSH 2024, NIOSH, *Mining and Ground Falls*, viewed 9 October 2024, https://www.cdc.gov/niosh/mining/topics/ground-falls.html

Ortlepp, WD 1983, 'Considerations in the design of support for deep hard-rock tunnels', *Proceedings of the 5th International Congress on Rock Mechanics*, Australian Geomechanics Society, Melbourne, pp. D179–187.

Potvin, Y, Wesseloo, J & Heal, D 2010, 'An interpretation of ground support capacity submitted to dynamic loading', in M Van Sint Jan & Y Potvin (eds), *Deep Mining 2010: Proceedings of the 5th International Seminar on Deep and High Stress Mining*, Australian Centre for Geomechanics, Perth, pp. 251–272, https://doi.org/10.36487/ACG_repo/1074_18

Zhang, P & Eriksson, F 2023, 'Assessment of static performance of welded mesh along mesh overlap used at Kiirunavaara mine', *IOP Conference Series: Earth and Environmental Science*, vol. 1124, no. 012093.